J Mater Sci (2007) 42:3353–3357
DOI 10.1007/s10853-006-0905-y

SIZE-DEPENDENT EFFECTS

Iron-based composite oxides as alternative negative electrodes for lithium-ion batteries

I. Uzunov · S. Uzunova · D. Kovacheva · S. Vasilev · B. Puresheva

Received: 21 April 2006 / Accepted: 30 August 2006 / Published online: 26 April 2007

Abstract Nanosized lithiated iron oxides with 10 and 50 wt.% SiO_2 were prepared by a sol–gel method using 1 M $Fe(NO_3)_3 \cdot 9H_2O$ and 1 M $LiNO_3$ aqueous solutions in a stoichiometric ratio of 1:1 and colloidal silica. Dried xerogel was calcinated at 700 °C for 4 h in air. The X-ray data of samples synthesized using 10% and 50% SiO_2 showed the presence of a mixture of two phases: α-$LiFeO_2$ and $Li_{1-x}Fe_5O_8$ ($0 < x \leq 0.1$) for a sample containing 10% SiO_2 and $LiFe(SiO_3)_2$ and Fe_2O_3 (h) for a sample with 50% SiO_2. The electrochemical behaviour of the compounds was investigated galvanostatically within the 0.01–3.0 V range at a current density of 0.80 mA cm^{-2}. The $Li/Li_xFe_yO_z$ (10%) · SiO_2 cell showed a high initial reversible capacity of 1,080 mA h g^{-1} and a capacity of 600 mA h g^{-1} at the 30th cycle. Accounting these results is the presence of a SiO_2 phase which stabilizes the structure of the active mass on cycling.The mean charge voltage (1.8 V) and the discharge voltage of 1.0 V versus Li^+ reference electrode as well as the high reversible capacity indicate that this material is suitable for use as anode in lithium-ion batteries.

I. Uzunov (✉) · D. Kovacheva
Institute of General and Inorganic Chemistry, Bulgarian Academy of Sciences, 1113 Sofia, Bulgaria
e-mail: uzunov_iv@svr.igic.bas.bg

S. Uzunova · S. Vasilev · B. Puresheva
Institute of Electrochemistry and Energy Systems (Former CLEPS), Bulgarian Academy of Sciences, 1113 Sofia, Bulgaria

Introduction

In a search for new negative electrode materials for lithium-ion batteries to replace carbonaceous materials with respect to their limited capacity and low density, alternative systems such as lithium titanates, vanadates, amorphous composite tin oxide and composite alloys have been extensively studied [1–4].

From all the investigated metal oxides, the iron oxides have been relatively less studied, due to their low conductivity and frustrating cyclability. Nevertheless, the iron oxides are still thought to be one of the best candidates for active electrode materials by virtue of their environmental affinity, high volumetric specific characteristics and low price [5–13].

The subjects of our study are lithiated iron oxides used as anode materials for lithium-ion batteries. They have a high initial discharge capacity but poor cycling stability due to dusting of the material and contact waste between particles. The process is connected with the electrochemical reaction of lithiation, which differs from the classical Li insertion/deinsertion mechanism.

The first discharge causes irreversible destruction of the crystal framework, which leads to formation of metal nanoparticles (5–8 nm) dispersed in the amorphous lithium oxide. The reversible reaction is related to the formation and decomposition of Li_2O accompanied by a reduction/oxidation process of the nanoparticles [5, 13]. Consequently, the cycling stability of lithiated iron oxides depends on the uniform and homogeneous distribution of the iron ions in lithium oxide matrix and the degree of precursor disintegration. Different methods, such as doping with other transition metal ions, covering with oxides

etc. have been reported for stabilization of the active materials structure and improving their electrochemical behaviour during the charge/discharge process [14–17]. Chen et al. reported a templating method for synthesis of α-Fe_2O_3 nanotubes using alumina membrane [18]. It was established that the as prepared material exhibits high initial discharge capacity of 1,415 mA h g^{-1} and loss of capacity after 100th cycle about 36%.

In this paper we report a new approach to the improving of the electrochemical behaviour of lithiated iron oxides by including in the active material the amorphous silica. The latter forms a substantial matrix in which iron ions and LiO_2 have a homogeneous distribution with a good contact between the individual particles.

Experimental

Synthesis

In order to investigate the influence of silicon dioxide upon the structure and electrochemical behaviour of lithiated iron oxides, three samples were synthesized: sample A, sample B and sample C.

Samples were prepared by mixing of 1 M $LiNO_3$ and 1 M $Fe(NO_3)_3$ aqueous solutions in a stoichiometric ratio of 1:1(initial solution). Sample A was prepared by heating initial solution at 100 °C until evaporation of the water. The substance was calcinated at 700 °C for 4 h. The precursors of samples B and C were obtained by mixing the initial solution with 10 wt.% SiO_2 (sample B) and 50 wt.% SiO_2 (sample C) at room temperature and constant pH 9. The colloidal silica used for the synthesis consists of particles with average size of 10–20 nm and a density of 1.30 g cm^{-3}. Dried xerogels were calcinated at 700 °C over 4 h in air.

XRD and SEM characterization

Phase composition, morphology and particle size of the samples were determined by X-ray powder diffraction analysis (XRD) and scanning electron microscopy (SEM). X-ray analysis was carried out using a Philips ADP 15 diffractometer with Cu Kα radiation . The diffraction data were processed with the Powder Cell program to determine the approximate stoichiometry of the synthesized phases [19].

The morphology of the particles was investigated by SEM using a JEOL-Superprobe 733.

Electrochemical characterization

The electrochemical behaviour of the synthesized materials was investigated at room temperature in a three-electrode cell within the 0.01–3.0 V range during charge/discharge at a current density 0.80 mA cm^{-2} using a computer controlled laboratory cycling equipment. The negative electrode was a lithium foil. The electrolyte used was a mixture of 1 M $LiClO_4$–ethylene carbonate and dymethyl carbonate (EC/DMC) in a ratio of 1:1. The water content in the electrolyte was less than 30 ppm. The positive electrode composites were prepared from the active material (15 ± 2 mg) with teflonized acetylene black (TAB2) [20] in a weight ratio of 1:1. The obtained mass was pressed onto Cu-foils (15 mm diameter) at a pressure of 981 MPa. All assemblies were carried out in an argon filled dry box.

Results and discussion

Phase composition and microstructure

The X-ray patterns of samples A, B and C are shown in Fig. 1. The X-ray patterns of sample A and sample B contain the diffraction lines of two phases: approx. About 95% α-$LiFeO_2$ (cubic phase) and 5% $Li_{1-x}Fe_5O_8$

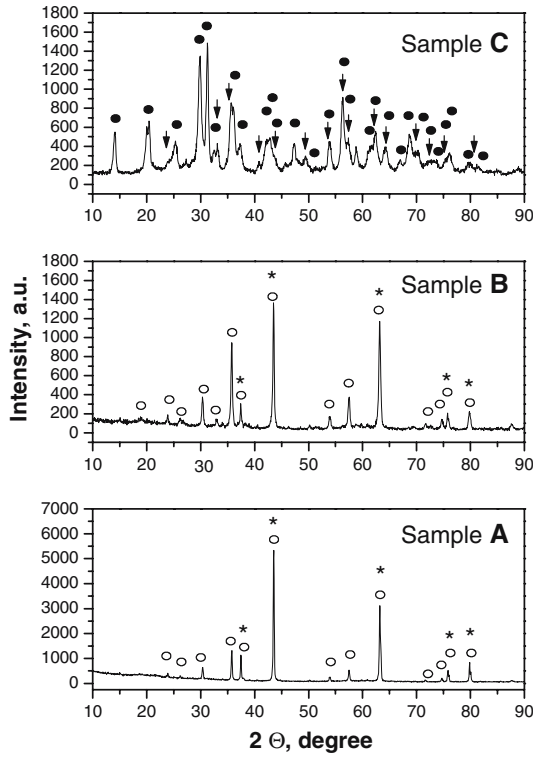

Fig. 1 XRD patterns of: sample A, sample B and sample C; (*) $LiFeO_2$; (○) $LiFe_5O_8$; (•) $LiFe(SiO_3)_2$; (↓) Fe_2O_3 (h)

($0 < x \leq 0.1$) (spinel phase) for sample A and 90% α-$LiFeO_2$ and 10% $Li_{1-x}Fe_5O_8$ ($0 < x \leq 0.1$) for sample B. The discrepancy between the initial quantity of lithium and its content in the final products can be explained by the loss of Li in the form of Li_2O during the calcination. The losses for sample A and sample B are at an average 14%, whereas for sample C the waste is 9%.

No diffraction lines of silicon dioxide were seen for sample B, which indicates that SiO_2 is presented in an amorphous state.

The X-ray patterns of sample C contain the diffraction lines of two phases: approximately 90% $LiFe(SiO_3)_2$ (pyroxene-type) and 10% Fe_2O_3 (h). The pyroxene monoclinic structure, SG *C*2/*c*, consists of single chains of tetrahedra extending along the *c* axis of the unit cell. The pyroxene formula unit M2 · M1 · T_2O_6 contains six oxygens and four cations: two in tetrahedral sites and one each in M1 and M2. The site preferences are as follows:

- T (tetrahedra): Si.
- M1 (small octahedron): Fe^{3+}.
- M2 (larger cation site): Li^+.

There are two types of cation positions, designated M1 and M2. The smaller M1 sites are situated between the apices of opposing tetrahedra, and are almost regular octahedra, which also form chains along the *c*-axis. M2 sites are larger. They lie between the bases of tetrahedra, and are more distorted 6- or 8-fold sites (Fig. 2). The parameters of the unit cell are, $a = 9.68$ Å, $b = 8.67$ Å, $c = 5.29$ Å, angle $\beta = 110.08°$ [21, 22].

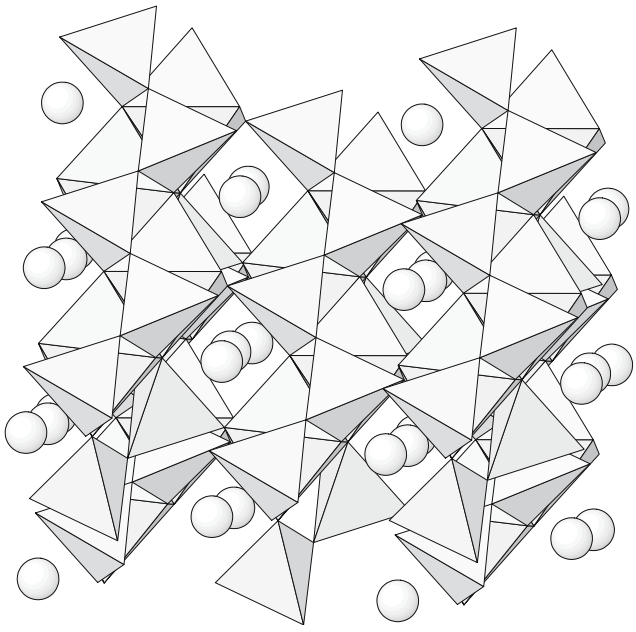

Fig. 2 Structure of pyroxene

The particle sizes of the three samples were determined by SEM investigations. The micrographs are presented in Fig. 3.

For three samples the particles possess prevailing spherical form. The particle sizes were found to vary within the range 100–150 nm (sample A), 80–120 nm (sample B) and 50–80 nm (sample C). The smaller particle size of samples B and C is due to the sol–gel preparation method. The particles of sample A are good pronounced and detached, while the particles of samples B and C are distributed homogeneously within the amorphous silica matrix.

Electrochemical behaviour

The charge/discharge curves after initial lithiation between 0.01 and 3.0 V of the Li/sample A, Li/sample B and Li/sample C cells and a current density of 0.80 mA h cm^{-2} are depicted in Fig. 4.

In comparison with Li/sample A the latter two cells show a decreased voltage discharge plateau from 1.15 to 1.0 V (for sample B) and from 1.15 to 0.75 V (for sample C).The electrochemical behaviour of the three cells during cycling is presented in Fig. 5. It can be seen that the discharge capacity drops during cycling.

The cell with pure $Li_xFe_yO_z$ electrode (sample A) displayed an initial reversible capacity of 580 mA h g^{-1}, while $Li_xFe_yO_z$ with 10 wt.% SiO_2 (sample B) presented a higher capacity (1,080 mA h g^{-1}) and $Li_xFe_yO_z$ with 50 wt.% SiO_2 (sample C) exhibited the lowest capacity (450 mA h g^{-1}).

The highest reversible capacity of 600 mA h g^{-1} during the 30th cycle was exhibited by the cell Li/sample B, and the worst capacity, 120 mA h g^{-1} was found with cell Li/sample C. The different electrochemical behaviours of the three cells are due to a difference in their composition and microstructure.

After the initial lithiation, in the case of sample A conditions which facilitate powdering of the active material and loss of contact between the particles are created, which results in a capacity loss. The higher discharge capacity for sample B is related to the formation of a steady microstructure with the participation of SiO_2, which prevents the dusting of the material during cycling with a minimum loss of contact between the active material particles. Additional investigations are needed for optimizing the silica content in the active material.

Sample C differs in structure from the other two samples. To our knowledge, there are no literature data from previous studies on the electrochemical activity of pyroxene. In the present case the electrochemical

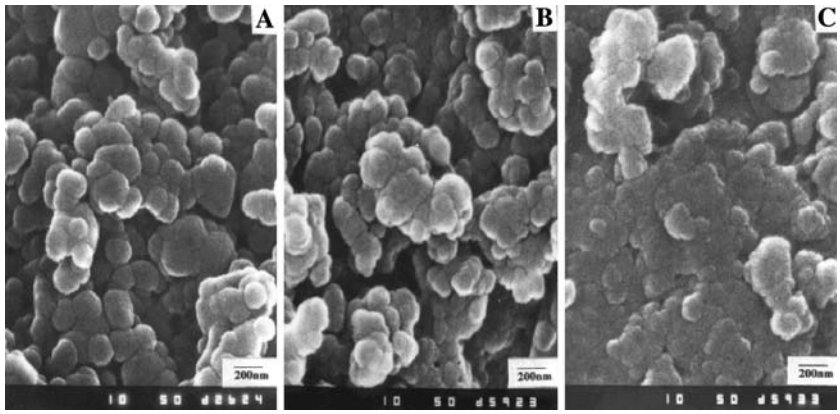

Fig. 3 Micrographs of: (**a**) sample A, (**b**) sample B and (**c**) sample C

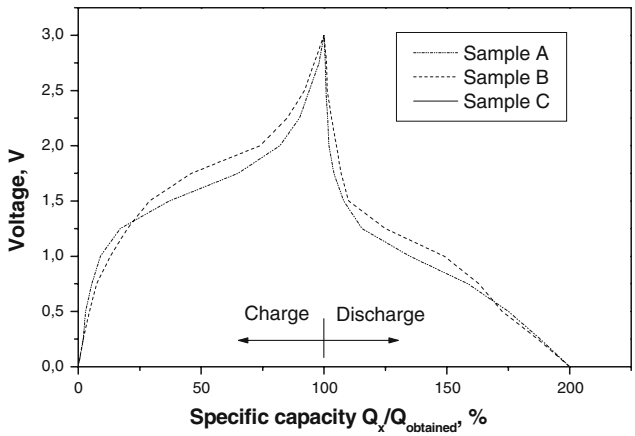

Fig. 4 The charge/discharge curves after initial lithiation of samples A, B and C

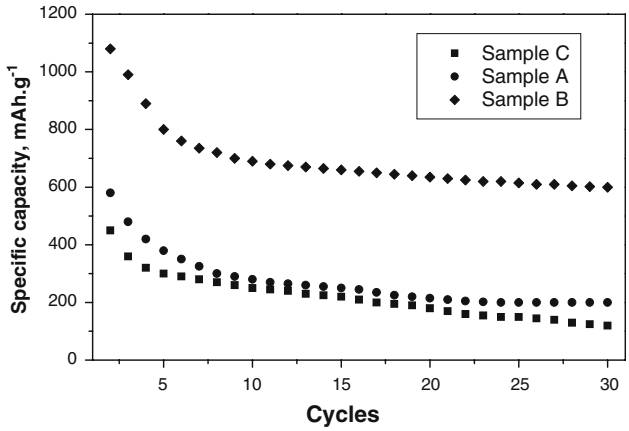

Fig. 5 Specific discharge capacity versus number of cycles for Li/samples A, B and C cells

activity of sample C cannot be explained by the presence of 10% Fe_2O_3 (h) alone.

In an effort to elucidate the mechanism of electrochemical interaction in the Li/sample A, Li/sample B and Li/sample C, within the range 0.01–3.0 V ex situ XRD investigations of electrodes after the first discharge and firs charge were carried out (Fig. 6).

After the initial lithiation of sample A and sample B, the peaks corresponding to Li_2O and finely dispersed iron with crystallites sizes below 5 nm were observed. After delithiation it was established the formation of an amorphous mass. Similar results were also obtained by Poizot et al. [13]. After the lithiation/delithiation process of sample C (pyroxene) a phase of α-Fe_2O_3 (h) was detected in X-ray patterns. It turns to the assumption that after initial lithiation the pyroxene

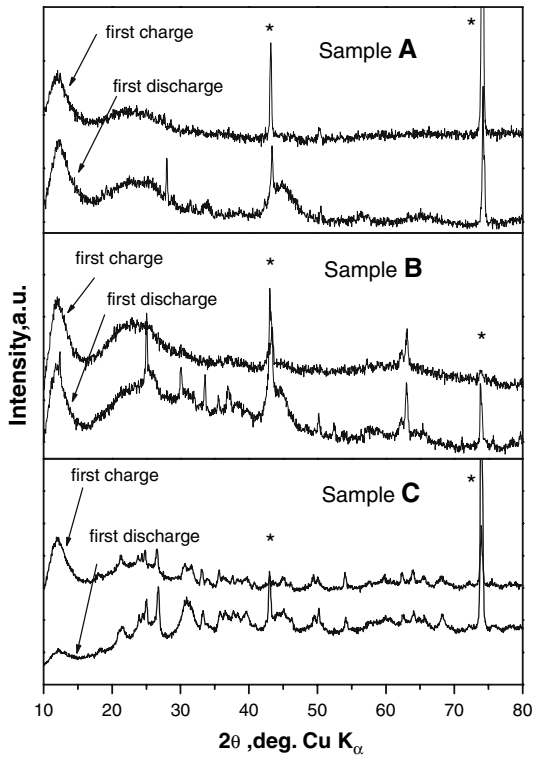

Fig. 6 Ex situ XRD patterns of electrodes (samples A, B and C) after the first discharge and firs charge

structure was destroyed and most probably some lithium-silicon phases were formed.

Further studies should be aimed at synthesizing a pure pyroxene phase and investigating its electrochemical behaviour at various voltage intervals.

Conclusions

A new approach to the synthesis of composite active materials including intimate mixing of three different inorganic substances is reported. The influence of an admixture of colloidal SiO_2 on microstructure and electrochemical behaviour of lithiated iron oxides was studied. Silicon dioxide was found to yield a homogeneous multi-component material which is steady during the cycling process. The material with 10 wt.% SiO_2 exhibited three times higher reversible capacity at the 30th cycle than the pure lithiated iron oxide. The results obtained advocate that colloidal silica is suitable for the microstructure stabilization of other active materials and should stabilize their electrochemical characteristics upon cycling.

Acknowledgements The authors gratefully acknowledge financial support by The Bulgarian Science foundation: Contract X-1412.

References

1. Winter M, Bezenhard JO, Spahr ME, Novak P (1998) Adv Mater 10:725
2. Behm M, Irvine JTS (2002) Electrochem Acta 47:1727
3. Idota Y, Kubota T, Matsufuji A, Maekawa Y, Miyasaka T (1997) Science 276:1395
4. Badway F, Plitz I, Grugeon S, Laruelle S, Dolle M, Gozdz AS, Tarascon J-M (2002) Electrochem Solid State Lett 5:A115
5. Obrovac MN, Dunlap RA, Sanderson RJ, Dahn (2001) J Electrochem Soc 148(6):A576
6. Lee YT, Yoon CS, Lee YS, Sun Y-K (2004) J Power Sources 134:88
7. Xu JJ, Jain G (2003) Electrochem Solid State Lett 6(9):A190
8. Tabuchi M, Ado K, Sakaevbe H, Masquelier C, Kageyama H, Naklamura O (1995) Solid State Ionics 79:220
9. Shirane T, Kanno R, Kawamoto Y, Takeda Y, Kamiyama T, Izumi F (1995) Solid State Ionics 79:227
10. Kanno K, Shirane T, Kawamoto Y, Takeda Y, Takano M, Ohashi M, Yamaguchi Y (1996) J Electrochem Soc 143:2435
11. Liu H, Wu YP, Rahm E, Holze R, Wu HQ (2004) J Solid State Electrochem 8:450
12. Thackeray MM, David WIF, Goodenough JB (1982) Mat Res Bul 17:785
13. Poizot P, Laruelle S, Gugeon S, Dupont L, Tarascon J-M (2000) Nature 407:496
14. Lee YS, Sato S, Sun YK, Kobayakawa K, Sato Y (2003) Electrochem Commun 5:359
15. Abraham KM, Pasquariello DM, Willstaedt EB (1990) J Electrochem Soc 137(3):743
16. Kim J, Manthiram A (1999) J Electrochem Soc 146(12):4371
17. Choi S, Manthiram A (2002) J Electrochem Soc 149(5):A570
18. Chen J, Xu L, Li W, Gou X (2005) Adv Mater 17:582
19. Kraus W, Nozle G (2000) Power cell program for Windows Ver.2.4. BAM, Berlin
20. Manev V, Momchilov A, Tagawa K, Kozawa A (1993) Prog Batteries Battery Mater 12:157
21. Klein C, Hurlbut Jr CS (1999) In: Manual mineralogy (after JD Dana). Wiley, New York, p 682
22. Pommier C, Downs R, Stimpfl M, Redhammer G, Bonner Denton M (2005) J Raman Spectrosc 36:864